Geoderma 152 (2009) 43–52

Contents lists available at ScienceDirect

Geoderma

journal homepage: www.elsevier.com/locate/geoderma

Modelling the three-dimensional spatial distribution of soil organic carbon (SOC) at the regional scale (Flanders, Belgium)

J. Meersmans [a,*], B. van Wesemael [a], F. De Ridder [b], M. Van Molle [c]

[a] Geography Department, Université Catholique de Louvain, Place Louis Pasteur 3, 1347 Louvain-la-neuve, Belgium
[b] VITO — Energy Technology, Boeretang 200, 2400 Mol, Belgium
[c] Geography Department, Vrije Universiteit Brussel, Pleinlaan 2, 1050 Brussels, Belgium

ARTICLE INFO

Article history:
Received 12 January 2009
Received in revised form 27 April 2009
Accepted 9 May 2009
Available online 25 June 2009

Keywords:
Soil organic carbon
Depth
Vertical distribution
Land use
Soil type
Belgium

ABSTRACT

The rate of exchange of CO_2 between the soil and the atmosphere depends on the stability of the organic carbon stored in the soil. Recent studies show that carbon stored in the subsoil is characterised by larger turnover times than the carbon stored in the topsoil. Consequently, identification of the depth at which high/low amounts of SOC are stored is essential for applying sustainable management of the soil in the light of global warming and related threats. This study investigates the depth distribution of SOC in relation to land use and soil type based on a large dataset for Flanders (Belgium). Soil type determines the SOC content along the entire profile. On the contrary, land use appears to have a strong influence on SOC content in the top layers of the profile, but doesn't play a significant role at the bottom of the profile (>1 m depth). SOC content near the surface of the profile is remarkably higher in fine (clay) textured soils than in coarse (sand) textured soils and tends to increase by increasing soil wetness under sand and silt textured soils. SOC at the bottom of the profile increases as well by increasing soil wetness, but only in fine (clay and silt) textured soils. The rate of decline of SOC content with depth depends on texture and land use. Under forest this decline is remarkably fast, although less so in the more sandy soil types. The overall model predicts the distribution of SOC density by depth using land use and soil type information and allows in its integrated form the estimation of SOC stocks that can be represented on SOC maps until a reference depth free of choice. Applying this model, based on a three-dimensional spatial distribution approach, the total amount of SOC stored in Flanders is calculated at 62.20 ± 0.72 Mt C for the top 0.3 m and 103.19 ± 1.27 Mt C for the top 1 m.

1. Introduction

The soil organic carbon (SOC) pool is considered as one of the most important reservoirs of the global C-cycle (e.g. Bohn, 1982). This reservoir has the potential to act as a major source or sink of greenhouse gases due to its large extent and active interaction with the atmosphere (Gal et al., 2007). Negative impacts of human activities on global warming, soil degradation and desertification can be limited by improved soil management, encouraging the enhancement of soil C sequestration (Milne et al., 2007). As a consequence, the localisation of environments determined by low/high SOC stocks at (sub)national level (i.e. the scale where the policy maker acts) is of great importance. In addition, organic matter is directly related to soil quality and has a major influence on soil structure, water holding and cation exchange capacity. Consequently, SOC content is used as an indicator for soil quality (e.g. Andrews et al., 2004; Dawson et al., 2007; Pattison et al., 2008). For example, high soil organic carbon content appears to diminish eutrophication or contamination risks of the groundwater or nearby ecosystems due to nitrate (NO_3^-) or pesticide leaching (e.g. Gundersen et al., 1998; Dousset et al., 2004; Poissant et al., 2008). Within this context, the vertical distribution of organic matter appears to be important, as SOC in the subsoil shows to be strongly related to sorption capacity of pesticides and to denitrification capacity of leached components (e.g. Lafrance and Banton, 1995; Richards and Webster, 1999). These findings underline the importance of mapping SOC distribution (with depth) at the regional scale as this information can be used as input for models estimating the spatial pattern of potential groundwater contamination by pesticides or nitrate leaching (e.g. Lindahl et al., 2005; Jarvis et al., 2007).

The most common approach to map SOC at the regional scale is to stratify the study area by land use and/or soil type, to calculate mean SOC stocks by land use and/or soil type combination and then attribute this value to the corresponding polygons/grid-cells on the map (e.g. Kern, 1994; Batjes, 2000; Liebens and VanMolle, 2003; Lettens et al., 2005). Due to the great spatial heterogeneity of the landscape some of these classes are limited in space or not easily accessible and therefore risk having few or no SOC data. Consequently, following the traditional method no reliable mean SOC value can be predicted for these classes. Nevertheless, these classes are most often representing extreme environments with extreme (high or low) SOC contents. This implies

* Corresponding author. Place Louis Pasteur 3, 1348 Louvain-la-Neuve, Belgium. Tel.: +32 10/47 28 80; fax: +32 11/47 28 77.
E-mail address: jeroen.meersmans@uclouvain.be (J. Meersmans).

0016-7061/$ – see front matter
doi:10.1016/j.geoderma.2009.05.015

that these zones have an important contribution to the spatial distribution and that the absence of reliable SOC values for these classes forms an important source of uncertainty. In more recent studies, a model predicting map unit specific SOC values was used in order to overcome this problem (e.g. Jones et al., 2004; Cerri et al., 2007; Milne et al., 2007; Meersmans et al., 2008). To obtain a more complete and detailed spatial distribution Jones et al. (2004) used a pedo-transfer rule, defined as a series of 'if-then' conditions and with soil, land use and climate as input variables, while Meersmans et al. (2008) constructed a regression model to predict SOC by land use, texture and drainage combination. The latter study showed that no (reliable) predictions could be made for large areas of poorly drained valley soils by using the traditional mean approach. Consequently, the total area for which (reliable) SOC stocks could be calculated increased by 8.1% and the total predicted SOC stock increased by 10.1% by applying the model instead of the traditional approach. Milne et al. (2007) developed the 'Global Environment Facility Soil Organic Carbon (GEFSOC) modelling system' to map future SOC stock changes at the national and sub-national scale. This modelling approach was applied in Jordan (Al-Adamat et al., 2007), Brazilian Amazon (Cerri et al., 2007), Kenya (Kamoni et al., 2007) and the Indian part of the Indo Gangetic plains (Bhattacharyya et al., 2007).

Many studies investigated the influence of physical soil properties on SOC and/or calculated total SOC storage at regional scale considering a fixed soil depth, e.g. top 0.3 or 1.0 m (Feller and Beare, 1997). Consequently, these studies do not contain information on the vertical distribution of SOC and are missing the depth or 3rd dimension of the spatial distribution. Nevertheless, knowledge on the depth distribution of soil organic carbon (SOC) is very important to understand how this reservoir acts in the global C cycle and in particular to have an insight into the soil–atmosphere interaction. In order to investigate the SOC distribution with depth, some studies grouped their measurements into fixed depth increments (e.g. Jackson et al., 2000; Slobodian et al., 2002; Omonode and Vyn, 2006), while others fitted continuous functions through the data. Thereby, the exponential decline is most frequently used (e.g. Hilinski 2001; Sleutel et al., 2003). The factors determining the SOC distribution with depth are various. Different studies showed that root biomass declines faster with depth than SOC (e.g. Gill et al., 1999; Jobbagy and Jackson, 2000). This should be the consequence of a downwards C transport within soil profile or lower decomposition rates of organic material in deeper layers. On the one hand, seepage water transport, texture related soil permeability, earthworm bioturbation, leaching and vertical soil mixing by organisms were identified in previous studies as the most important factors determining the vertical transport of SOC (Jobbagy and Jackson, 2000; Don et al., 2007). On the other hand, radiocarbon studies illustrate an increase in turnover time and stability of SOC with increasing depth (e.g. Trumbore, 2000; Baisden and Parfit, 2007). Fontaine et al. (2007) considered the lack of energy supply of microbes in deeper soil layers, under the form of fresh organic matter as the main explanatory factor for this phenomenon. Thus, defining the depth at which important SOC densities are present indicates the stability of the carbon stored in the soil. In other words, SOC information by depth provides information on the likelihood of the soil to exchange CO_2 with the atmosphere.

This study aims to construct an empirical model describing depth distribution of soil organic carbon (SOC) in relation to texture, drainage and land use for Flanders (Belgium) in order to analyse the spatial distribution of SOC density in three dimensions and to produce SOC stock maps until a reference depth to be chosen by the user.

2. Material and methods

2.1. Study area

Flanders is situated in the northern part of Belgium, a country in the north-west of Europe, and covers an area of 15,521 km^2. Given the rather small size and the absence of important variation in altitude, this region is characterised by uniform climate conditions, with an annual precipitation amount of 700 to 800 mm and a mean temperature of 9 to 10 °C. Nevertheless, one can find a variation in soil types in Flanders: fertile loess soils in the south (Luvisol), sand textured soils in the north (Podzols) and wet clay rich soils (Fluvisols) in the alluvial and coastal plains in the west. As the region is densely populated, the area is dominated by agricultural and urban land use types.

2.2. SOC data

The model has been developed based on the dataset 'Aardewerk', containing almost 7000 profiles pits sampled throughout Flanders during the Belgian National Soil Survey (1947–1974). 75% of the data was used to calibrate the model. The other 25% of the data were used for validation. The profiles in the dataset were provided with information on land use, texture and drainage class, classified according to the Belgian soil classification system (Fig. 1 and Table 1). No information on land use history of the sites was reported. In most of these profiles, the soil is described until a depth of 1–1.5 m, and contains 5 to 6 horizons. For each horizon the depth, the percentages of sand, silt, clay, as well as the SOC concentration (g C kg^{-1}), determined by the classic bichromate method of Walkley and Black (1934) are given (Van Orshoven et al., 1988). In order to compensate the incomplete oxidation of carbon characteristic for the Walkley and Black method, a correction factor of 1.33 is applied. SOC mass densities (kg m^{-3}) are obtained by multiplying the SOC mass concentration (g C kg^{-1}) by soil bulk density (kg m^{-3}) (Eq. (1)):

$$\mathrm{SOC} = \rho_S{*}\frac{C}{1000} \tag{1}$$

where:

SOC SOC mass density of the sample (kg C m^{-3})
ρ_S bulk density of the soil (kg m^{-3})
C SOC concentration of the sample (g C kg^{-1}).

As bulk density information is not provided by 'Aardewerk', a pedo-transfer function (PTF) is used to predict this soil property for each sample. The use of a PTF risks to over/underestimates real bulk density and creates a source of uncertainty in calculating SOC mass

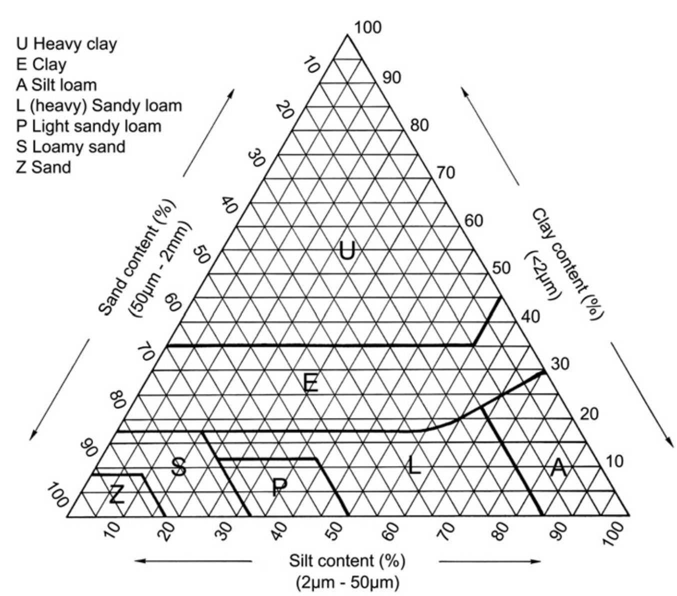

Fig. 1. Belgian soil texture classification triangle (after Ameryckx et al., 1995).

Table 1
Belgian drainage classification system as a function of the soil texture (heavy clay (U), clay (E), sandy loam (L), silt loam (A), light sandy loam (P), loamy sand (S), sand (Z); see Fig. 1 for the Belgian texture triangle) after Ameryckx et al. (1995).

Drainage class	Definition		Depth oxidation horizon (m) (min. depth water table)		Depth reduction horizon (m) (max. depth water table)
	Belgian system[a]	USDA drainage class[b]	Text. A, L, E, U	Text. Z, S, P	
a	Very dry	Excessively	–	–	–
b	Dry	Well	>1.2	0.9–1.2	–
c	Moderately dry	Moderately-well	0.8–1.2	0.6–0.9	–
d	Moderately Wet	Moderately	0.5–0.8	0.4–0.6	–
h	Wet	Moderately-poorly	0.3–0.5	0.2–0.4	–
i	Wet	Poorly	0–0.3	0–0.2	–
e	Wet with reduction horizon	Moderately-poorly	0.3–0.5	0.2–0.4	>0.8
f	Very wet with reduction horizon	Poorly	0–0.3	0–0.2	0.4–0.8
g	Extremely wet	Very poorly	0	0	<0.4

[a] Ameryckx JB, Verheye W, Vermeire R (1995) *Bodemkunde*, Gent.
[b] Soil Survey Staff (1951) *Soil Survey Manual*, United States Department of Agriculture, U.S. Dept. Agricultural Handbook, 18, Washington, D.C.

density. Nevertheless, Boucneau et al. (1998) compared different pedo-transfer functions (PTF's) predicting soil bulk density for Flemish soils. They showed that, of all PTF's (applicable in this study) the general PTF of Manrique and Jones (1991), has the best correlation between observed and predicted bulk density values. Consequently this function, with a minimal value of 0.3 g cm^{-3} (i.e. value corresponding to peat soils (Lettens et al., 2004)), is used in this study to predict bulk density (g cm^{-3}) for each sample (Eq. (2)).

$$\rho_S = 1.66 - 0.318^* \sqrt{\frac{C}{10}} \tag{2}$$

2.3. Land use and soil type maps

The study area was stratified by an overlay of the digital land use map of Flanders with the soil map of Belgium. The digital land use map of Flanders, with a resolution of 15 m, was derived from Landsat7-ETM+ images of the year 2001. Classification of these images combined with external road and waterway information resulted into 18 land use classes (OC GIS Vlaanderen, 2002). For the present study, four aggregated classes were extracted from the digital land use map of Flanders: i.e. forest, grassland, cropland and heath.

The digital soil map of Belgium is derived from the National Soil Survey (1947–1974) (OC GIS Vlaanderen, 2001). From the soil codes on this map information concerning drainage and texture class could be extracted. Fig. 1 illustrates that Belgian soil texture classes were defined according to clay, silt and sand content. Whereas Table 1 shows that the Belgian soil drainage class system is based on the depth of occurrence of oxidation and reduction properties in the soil profile. These depths correspond to the minimum and maximum depth of the ground water during the year, or the position of the ground water table in winter and summer, respectively (Ameryckx et al., 1995). Consequently, Belgian texture and drainage classification systems allow production of numeric maps presenting variables related to these properties, i.e. regarding texture: clay, silt, and sand content as well as geometric mean particle size (Dg) and considering drainage: maximal and minimal depth of the ground water table. As drainage information was not updated for current situation, inventories of the SOC database correspond to the one of digital soil map, which is important to clearly identify the influence of different soil properties on SOC distribution with depth.

2.4. SOC depth distribution

SOC depth distribution in the tillage layer differs from the deeper layers. The SOC density remains constant until the tillage depth (td) is reached. At greater depth, SOC density shows an exponential decline with depth (Eq. (3)):

$$\begin{aligned} z < \mathrm{td} &: \mathrm{SOC}(z) = \mathrm{SOC_{surf}} \\ z > \mathrm{td} &: \mathrm{SOC}(z) = A \cdot e^{\alpha \cdot (z-\mathrm{td})} + \mathrm{SOC}_\infty \end{aligned} \tag{3}$$

where:

z	depth (m)
td	tillage depth (m)
$\mathrm{SOC}(z)$	SOC mass density at depth z (kg C m^{-3})
$\mathrm{SOC_{surf}}$	SOC mass density (kg C m^{-3}) at the surface
SOC_∞	SOC mass density (kg C m^{-3}) at the bottom of the soil profile.

α is a constant which determines the shape of the exponential part of the curve.

$$A = \mathrm{SOC_{surf}} - \mathrm{SOC}_\infty \tag{4}$$

When the model is applied to permanent grassland, forest or heath, Eq. (3) can be simplified to an exponential relation:

$$\mathrm{SOC}(z) = A \cdot \exp^{\alpha \cdot z} + \mathrm{SOC}_\infty. \tag{5}$$

In order to obtain a realistic tillage depth (td), different model simulations were performed for cropland. For each simulation the data was divided in two groups: i.e. one group with samples near the surface to fit the constant part of the model and another group, containing all deeper samples, to fit the exponential decline at greater depth. In each simulation the amount of samples in the first group increased and in the second group declined one at the time. The simulation with the best fit was retained. From the selected simulations the tillage depth (td) is determined by the intersection of the constant and exponential parts of the curve (Eq. (6)). More detailed explanation and a graphical example of this method can be found in Meersmans et al. (in press).

$$\mathrm{td} = \frac{\ln\left(\frac{(\mathrm{SOC_{surf}} - \mathrm{SOC}_\infty)}{A'}\right)}{\alpha} \tag{6}$$

where

A'	extrapolated SOC(0) of the exponential part of the model — SOC_∞.

2.5. SOC mass

To calculate SOC mass per surface unit (kg C m^{-2}) until a certain reference depth (rd) Eq. (3) is integrated and results in Eq. (7):

$$\mathrm{SOC_{mass}} = \mathrm{SOC_{surf}} \cdot \mathrm{td} + \frac{A \cdot \left(e^{\alpha \cdot (\mathrm{rd}-\mathrm{td})} - 1\right)}{\alpha} + \mathrm{SOC}_\infty \cdot (\mathrm{rd} - \mathrm{td}). \tag{7}$$

Fig. 2 presents the methodological flowchart of this study. After grouping the data by land use–soil type class, the model (Eq. (3)) was fitted through the SOC depth data for all land use–soil type classes with more than 30 samples (Fig. 3). This resulted into a set of SOC_∞, A,

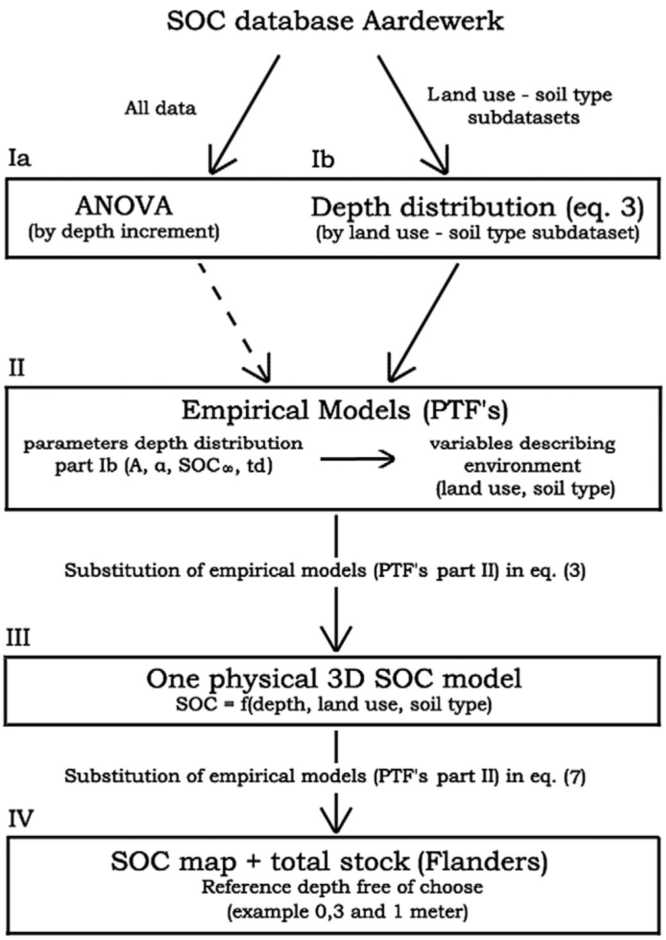

Fig. 2. Flowchart of the methodology.

td and α parameter values for each environment, which allows construction of a PTF for each parameter of the depth distribution function (Eq. (3), A, SOC_∞, α, td) by expressing the parameter as a function of land use, drainage and soil texture variables. To obtain one physical model describing depth distributions of SOC as a function of land use and soil type, the resulting pedo-transfer functions, are substituted in Eq. (3). Furthermore, substitution of these four PTF's in Eq. (7), i.e. the integrated form of the depth distribution model, combined with digital land use and soil type maps of the study area allows calculation of the total amount of carbon stored in the study area. By integrating the depth distribution function until certain depth of interest, the reference depth will be chosen by the user.

2.6. Software

For the modelling part of this research Matlab version 7.3 (MathWorks, Natick, Massachusetts, USA) was used. Statistical analyses were carried out in SPSS 11.0 (SPSS Inc., Chicago, Illinois, USA).

3. Results and discussion

3.1. ANOVA by depth increments

As expected, the results of ANOVA tests after grouping the data by 20 cm depth increments indicate that the influence of land use on SOC density decreases with depth, as land use has significant effect ($p = 0.001$) on SOC in the top layers, but not in the subsoil (>80 cm; Table 2). Texture and drainage, on the other hand, have a significant ($p = 0.001$) effect on the SOC content throughout the profile. Moreover, the interaction between texture and drainage is significant ($p = 0.001$) for all depths, which indicates that the effect of texture on

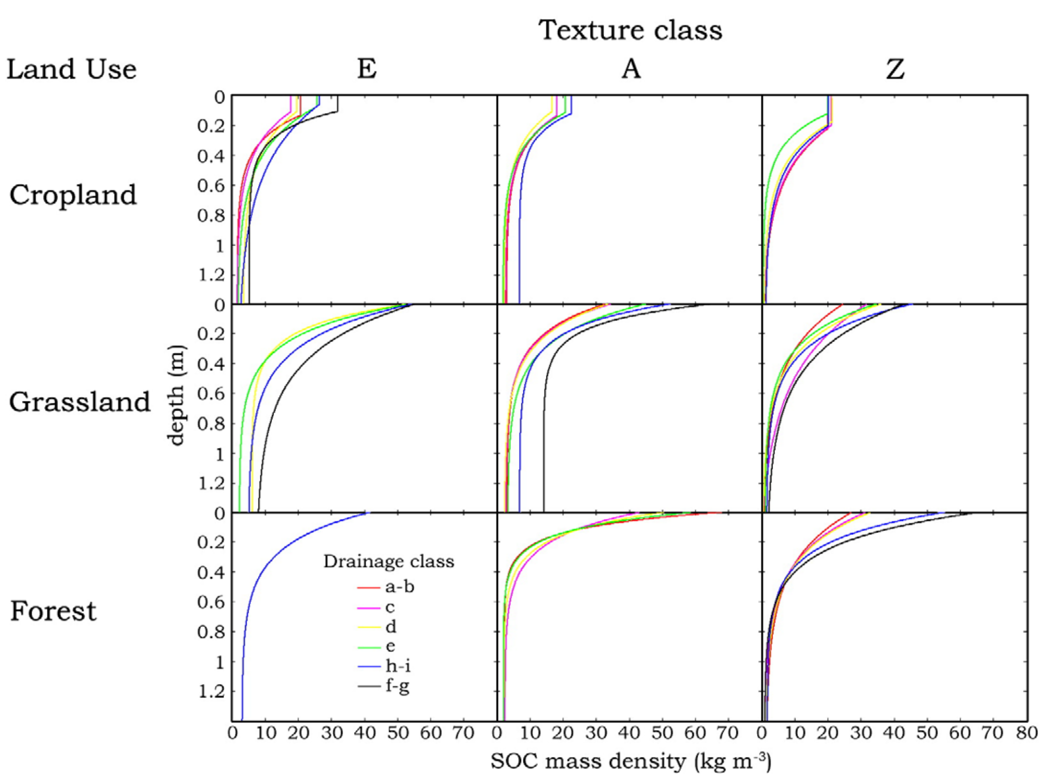

Fig. 3. Depth distribution model (Eq. (3)) applied on different land use–drainage class combinations within clay (E), silt-loam (A) and sand (Z) textured soils (n>30). A complete figure whereby the model is applied on all land use–soil type combinations of database Aardewerk (n>30) can be obtained from following website (i.e. E-Figure 1): www.jeroenmeersmans.be/research/publications/depth3Dmod.

Table 2
ANOVA results, testing the influence of land use (LU), texture (TXT), drainage (DR) and interactions on the SOC stocks by depth increments of 0.2 m at 3 different levels of significance: $0.01<p<0.05$ (*), $0.01<p<0.001$ (**) and $p<0.001$ (***) (*N* indicates the number of samples).

Depth (m)	(*N*)	LU	TXT	DR	LU*TXT	LU*DR	TXT*DR	LU*TXT*DR
0–0.2	(5384)	***	***	***	***	***	***	**
0.2–0.4	(4645)	***	***	***		*	***	
0.4–0.6	(4417)		***	***	**	***	***	
0.6–0.8	(3836)	**	***	***	*	***	***	
0.8–1.0	(3292)		***	***	*	***	***	
1.0–1.2	(2540)	*	*	***		*	***	
1.2–1.4	(3216)		***	***			***	
>1.4	(1758)		***	***			***	

SOC density depends on the drainage status (and visa versa) for all depths. These trends are in agreement with the ones of Jobbagy and Jackson (2000) who showed that the SOC content at the surface (0–20 cm) appears to be dominated by land use and climate, i.e. strong positive relation with precipitation and negative relation with temperature. While in contrast, SOC shows the highest correlation with clay content in deeper layers (1–3 m).

3.2. Depth distribution model

The depth distribution model (Eq. (3)) was applied for all land use–soil type combinations with at least 30 samples (E-Figure 1; Meersmans, 2008). Each graph shows the SOC depth distributions of different drainage class groups within one land use–texture class combination. A selection of some land use (i.e. cropland, grassland, forest)–texture classes (i.e. clay (E), silt loam (A) and sand (Z)) of E-Figure 1 is given in Fig. 3. From this figure one can observe immediately the general known trends to have higher SOC mass density values under more humid and/or fine textured soils and that under cropland tillage diminish considerably SOC content in the top layer (e.g. Tan et al., 2004; Zinn et al., 2005). By investigating the depth distribution instead of SOC content until fixed depth, we were able to identify the depth of specific relationships between these soil variables and the SOC content. Therefore these environmental variables will be discussed in detail for each parameter of the general SOC distribution model (Eq. (3)).

3.2.1. PTF A-parameter

The results show that topsoil SOC is highest under forest and lowest under cropland in almost all land use–soil type combinations (Fig. 3, E-Figure 1). This is in accordance with the literature and explained by the fact that forests have a relative higher above ground allocation of organic material as compared to other land uses. This results in a higher input of SOC at the surface due to litter fall under forest (Wang et al., 2004). Moreover, recent research pointed that difference in land management practises could affect seriously the distribution of SOC with depth. Under cropland, tillage declines the SOC stock in the top layer by exposing periodically the organic matter that is physically protected in micro-aggregates to biodegradation (Balesdent et al., 2000). Under grassland, the SOC mass densities near the surface tend to increase with decreasing particle size (i.e. higher clay or silt content). This is in agreement with other studies reporting a positive linear relation between clay or clay + silt content and SOC content until fixed reference depth (e.g. Zinn et al., 2005). A positive relation between soil wetness and SOC mass density near the surface can be observed in the sand and silt textured grassland soils (A, L, P, S, and Z). This trend was not found under clay textured soils (E, U) (Fig. 3, E-Figure 1). Davidson (1995) underlines as well the importance of drainage status on SOC by showing that SOC content increases with soil wetness. The relation between SOC mass near the surface and soil type is different for cropland and grassland. Under cropland the heavier soils (E, U, L) show a positive relation between SOC mass density near the surface and soil wetness, whereas this trend cannot be observed in sand and silt loam soils (A, Z) (Fig. 3, E-Figure 1). As the *A*-parameter is strongly correlated with the SOC mass density near the surface (i.e. correlation coefficient between *A* and SOC_{surf} of 0.851 for cropland, 0.966 for grassland, 0.999 for forest and 0.999 for heath, data not shown) the extracted topsoil SOC trend information is very useful to construct the PTF describing the *A*-parameter (Eq. (3)) as function of land use and soil type. The PTF contains 3 different land use specific equations (Eq. (8)), because of the strong land use dependency of the SOC mass density near the surface and their relation with soil type:

$$\begin{aligned} A_{\text{grassland}} &= H_2O_s{*}\left(a{*}\text{silt}^2 + b{*}\text{silt}\right) + c{*}H_2O_s{*}\text{sand} \\ &\quad + d{*}H_2O_w + e{*}\text{clay} + f \\ A_{\text{cropland}} &= g{*}H_2O_s{*}(\text{clay} + \text{silt}) + h{*}\text{sand}^2 + i{*}\text{sand} + j{*}\text{clay} + k \\ A_{\text{forest/health}} &= l{*}H_2O_s + m{*}\text{Dg} + n \end{aligned} \tag{8}$$

where:

H_2O_s	height of the deepest ground water table position (summer) above 1.5 m depth (m)
H_2O_w	height of the shallowest ground water table position (winter) above 1.5 m depth (m)
sand	sand content (%)
clay	clay content (%)
silt	silt content (%)
Dg	geometric mean particle size diameter (mm).

The corresponding R^2 value of the model is 0.81 for all environments, with land use specific values of 0.60 for grassland, 0.61 for cropland and 0.50 for forest/heath. Fig. 4 compares for every land use–soil type combination the initially calculated *A*-parameter value by applying Eq. (3) with the predicted values based on the PTF (Eq. (8)). This figure illustrates that the *A*-parameter values under cropland are remarkably lower than under grassland, forest/heath.

3.2.2. PTF SOC∞-parameter

One can state that for sand and sand-loam (L, P, S, Z) soils for each drainage–land use combination the SOC mass density converges to zero near the bottom of the profile (SOC_∞), while for clay and silt loam soils, this value is remarkably higher and tends to increase with increasing soil wetness (Fig. 3, E-Figure 1). Within the same soil type no important differences in SOC_∞ could be observed between the

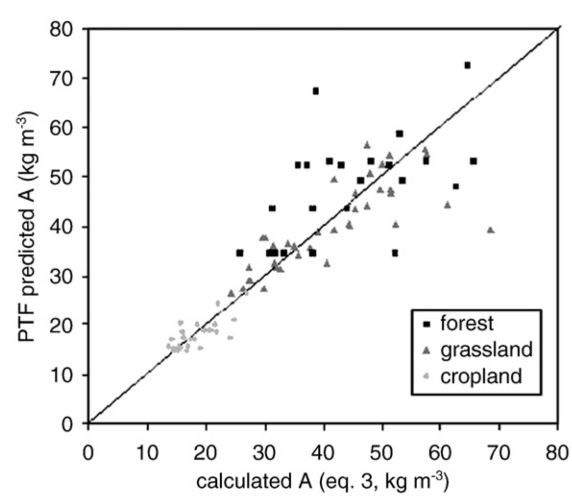

Fig. 4. Calculated (Eq. (3)) versus PTF predicted (Eq. (8)) *A* parameter (kg m^{-3}) for all land use–texture–drainage class combinations (Fig. 3).

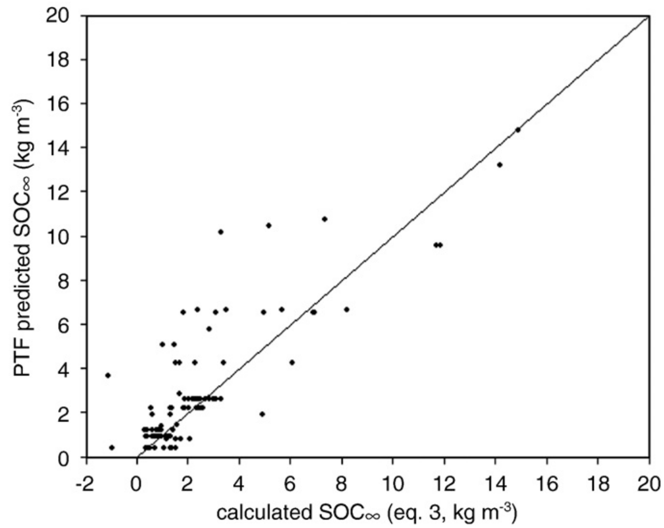

Fig. 5. Calculated (Eq. (3)) versus PTF predicted (Eq. (9)) SOC_∞ parameter (kg m^{-3}) for all land use–texture–drainage class combinations (Fig. 3).

different land uses. This corresponds to ANOVA analysis discussed earlier (Table 2). Moreover, the results lies in the line of the finding's reported by Jobbagy and Jackson (2000) showing that clay content controls SOC content in deeper layers. Consequently, a single relationship between SOC_∞ and soil type (i.e. texture and drainage) could be found. This resulted in one model, predicting SOC_∞, for all land uses (Eq. (9)). Moreover, the important interaction between texture (clay and silt content) and drainage (H_2O_s) on SOC stock at these depths is highlighted in the equation.

$$SOC_\infty = a*H_2O_s*clay + b*H_2O_s*silt + c*clay + d*silt \qquad (9)$$

The model (Eq. (9)) nicely describes the observed pattern with an R^2 value of 0.76 (Fig. 5).

3.2.3. PTF α-parameter

The rate of decline of SOC with depth in the exponential part of the depth distribution model (Eq. (3)) is represented by the α-parameter. As expected, the results show that forested soils are characterised by high SOC stocks near the surface and a strong decline of SOC with depth, while grassland soils have lower SOC stocks in top layers but higher stocks in deeper layers as a result of a weaker decline of SOC with depth

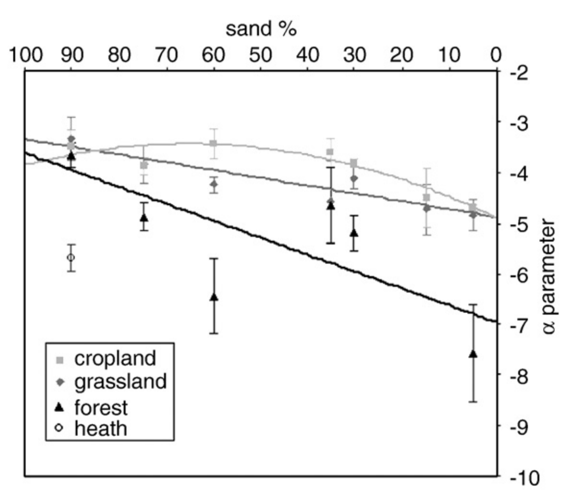

Fig. 6. Mean and standard deviation of calculated (Eq. (3)) and PTF predicted (line) (Eq. (10)) α parameter by sand content (%).

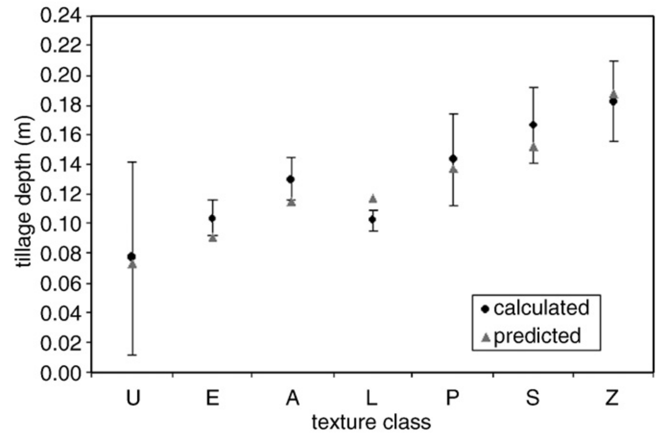

Fig. 7. Mean and standard deviation of calculated (Eq. (3)) versus PTF predicted (Eq. (11)) tillage depth by texture class (i.e. U: heavy clay, E: clay, A: silt loam, L: (heavy) sandy loam, P: light sandy loam, S: loamy sand, Z: sand).

(Fig. 3, E-Figure 1). This can be explained by the difference in below versus above ground allocation of living organic matter between both land uses. Mokany et al. (2006) measured for temperate climate root to shoot ratios of 0.20 ± 0.03–0.46 ± 0.06 under forest and 4.22 ± 0.52 under grassland. As under forest, almost all living organic material is stored above ground in the trees, the input of SOC mainly takes place at the surface due to fall of woody and relative slow decomposable debris. By way of contrast, under grassland the majority of the living organic material is stored below ground in the well developed root systems, which cause an important input of SOC in the subsoil from root turnover (Jobbagy and Jackson, 2000; Wang et al., 2004). Under sand textured soils the decline of SOC with depth in the subsoil is less pronounced than in heavier soils (Fig. 3, E-figure 1). This is counter intuitive as coarse textured soils are characterised by larger pores than fine textured soils and so have a higher oxidation capacity of SOC, resulting in a shorter

Table 3
Parameter values and 95% confidence interval of PTF's describing *A*, α, SOC_∞ and td as a function of land use and soil type (Eqs. (8)–(11)).

Parameter depth distribution model (Eq. (3))	Land use	Parameter PTF	Value	95% confidence interval	
A (kg m^{-3})	Grassland	*a*	0.0056	0.0020	0.0091
		b	−0.3269	−0.5945	−0.0592
		c	0.1454	0.0766	0.2143
		d	11.7340	9.1525	14.3154
		e	0.4135	0.3431	0.4839
		f	21.7186	19.5789	23.8584
	Cropland	*g*	0.1522	0.0823	0.2221
		h	0.0013	0.0010	0.0016
		i	−0.0665	−0.0925	−0.0406
		j	0.1304	0.0916	0.1691
		k	14.315	13.8036	14.8263
	Forest	*l*	42.3713	34.7906	49.9511
		m	−29.1021	−33.5331	−24.6710
		n	53.7206	51.4357	56.0054
α	Grassland	*a*	0.0155	0.0173	0.0138
		b	−4.8747	−4.7674	−4.9819
	Cropland	*c*	−0.0003	−0.0003	−0.0004
		d	0.0448	0.0504	0.0393
		e	−4.8863	−4.7907	−4.9819
	Forest	*f*	0.0337	0.0367	0.0308
		g	−6.9729	−6.7565	−7.1893
SOC_∞ (kg m^{-3})	All	*a*	0.0794	0.0112	0.1476
		b	0.1226	0.1033	0.1419
		c	0.1216	0.1121	0.1311
		d	0.0162	0.0147	0.0177
td (m)	Cropland	*a*	−0.0010	−0.0017	−0.0003
		b	0.1018	0.0709	0.1327
		c	0.1219	0.1103	0.1335

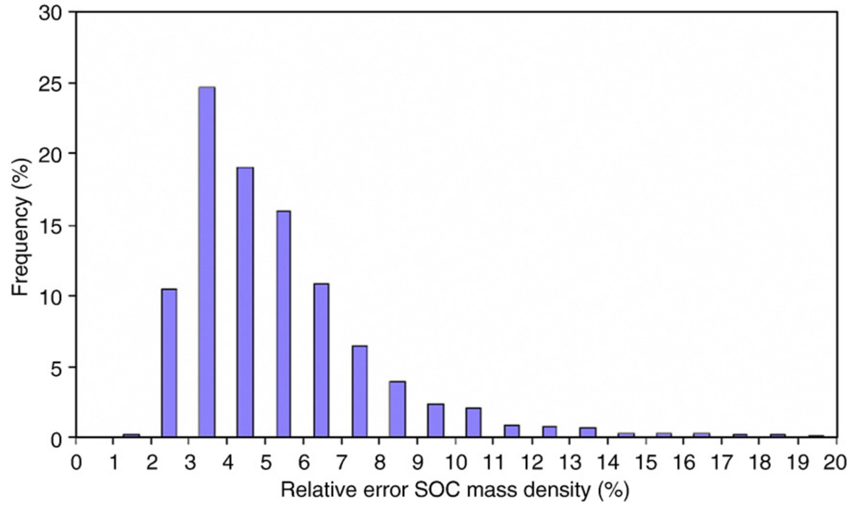

Fig. 8. Frequency distribution of the relative error on predicted SOC mass densities by applying the overall depth distribution model to different soil depths, land uses and soil type conditions.

turnover time. This implies that the slower decline of SOC with depth in sandy soils can not be the consequence of more stable conditions in deeper layers. An alternative explanation would be that vertical transport of SOC must be an important process for C accumulation at these depths. Don et al. (2007) stated that this process is stronger in profiles characterised by higher soil permeability. The results of our study confirm this, as the SOC decline with depth tends to slow down with increasing sand content, which suggests a stronger vertical SOC transport in soils characterised by larger pores or a higher permeability. The α-parameter is expressed in this study as a function of sand content in three different land use specific equations (Eq. (10)). Under grassland and forest the relation between the α-parameter and sand content could be described by linear functions. Under cropland the expression is more complex, as a quadratic function better describes the system.

$$\begin{aligned}\alpha_{grassland} &= a^*\text{sand} + b\\ \alpha_{cropland} &= c^*\text{sand}^2 + d^*\text{sand} + e\\ \alpha_{forest} &= f^*\text{sand} + g\end{aligned} \tag{10}$$

Fig. 6 illustrates the α-parameter by sand content and by land use class. The three land use specific models appear to converge to the same value (−3.5 to −4) for a sand content of 100%. As near all heath soils appear on sandy soils in Flanders (E-Figure 1), this land use could only be studied under Z textured sand (90% of sand). They are, with a mean α-parameter value of -5.7 ± 0.3, characterised by a very strong decline of SOC with depth. Despite the clear trends one can observe in Fig. 6, the proposed PTF has a rather low R^2 of 0.42, with R^2 values for the land use specific models of 0.23 for cropland, 0.20 for grassland, and 0.53 for forest.

3.2.4 PTF tillage depth

The calculated tillage depth (td) depends on texture. The mean tillage depth by texture class varies between 8 cm for heavy clay (U) and 19 cm for sand soils (Z; Fig. 7). This trend was expected and can be easily explained by the fact that the traction required for ploughing in fine textured soils (E, U, A) is much larger than in coarse textured soils (S, Z) and animals or tractors used in the 1960s were probably not powerful enough to plough the same depth in fine as in coarse textured soils. Increased mechanisation during the last 50 years allows deeper ploughing of the soil. As a consequence much deeper tillage should be expected nowadays, foremost in the fine textured soils. Van Meirvenne et al. (1996) recorded for northwest Belgium an increase in average tillage depth of almost 0.10 m between 1960 and 1990. Meersmans et al. (in press) showed that this increase in tillage depth in Belgian cropland soils is more pronounced under fine textured than coarse textured soils. They calculated an increase of 0.079 ± 0.031 m in silt loam (A) soils and 0.024 ± 0.050 m in sand (Z) soils for the period 1960–2006. Tillage depth is strongly correlated with Dg and clay content. This is shown by a correlation coefficient (r) of −0.65 and 0.69 respectively (data not shown). As the correlation between clay content and Dg was not too strong (<0.6) a linear combination of both texture variables is used to predict tillage depth (Eq. (11)).

$$\text{td} = a^*\text{clay} + b^*\text{Dg} + c \tag{11}$$

The corresponding R^2 value of the model is 0.57. Nevertheless, Fig. 7 illustrates that the predicted tillage depths using the model (Eq. (11)) are close to the observed mean tillage depths for each texture class.

3.3 Overall (land use–soil type) SOC depth distribution model

The substitution of the A, SOC_∞, td and α parameter PTF's (Eqs. (8)–(11)) in the depth distribution model (Eq. (3)) and calculation of SOC_{surf}

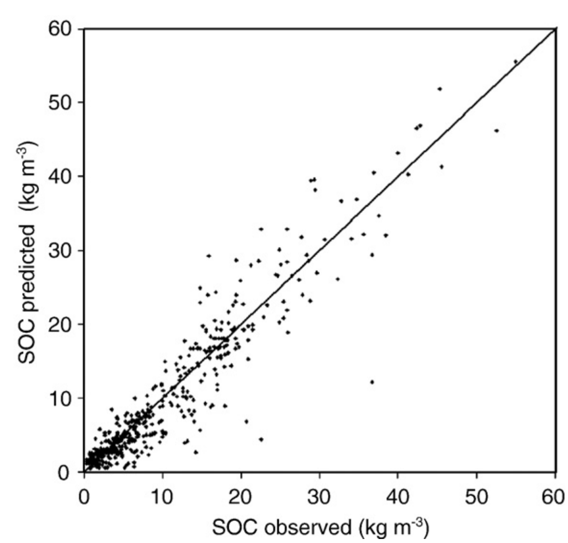

Fig. 9. Validation of the overall depth distribution model by comparing mean observed and predicted SOC mass densities (kg m^{-3}) of the validation sub-dataset. Each point represents a land use–soil type–depth increment (0.1 m interval) combination with at least 5 samples.

using Eq. (4), allows calculation of SOC density as a function of depth, land use and soil type. In other words the overall model allows generation of SOC distributions with depth for a given land use–soil type combination. The parameter values as well as their 95% confidence limits of this overall depth distribution model are given in Table 3. All parameters are significant at $p<0.05$ level.

3.3.1. Model uncertainty

In order to calculate the error on the estimated SOC mass density (kg m^{-3}) due to parameter uncertainty (Table 3) of this overall depth distribution model the Monte Carlo simulation technique was applied. Hereby, the model predicts the SOC mass density (kg m^{-3}) for each simulation by a set of parameter values randomly chosen from normal probability distributions with mean and standard deviation equal to the estimated value and 66.7% uncertainty (stdev) of the corresponding parameters. From all predictions, the standard deviation is used as error for the estimated SOC mass density (kg m^{-3}). The error on the estimated SOC mass density (kg m^{-3}) strongly depends on land use, texture, drainage and soil depth. Regarding the top 1 m, the relative value of this error ranges between 1.86% (for dry silt loam cropland soils in the tillage layer) and 28.65% (for extremely wet grassland at the soil surface). The majority (>80%) of the relative errors are between 2% and 7% (Fig. 8).

3.3.2. Model validation

To evaluate the quality of this overall (land use–soil type) depth distribution model we compared predicted and mean observed SOC mass density (kg m^{-3}) by land use–soil type–depth increment (0.1 m interval) combination with at least 5 samples from the validation set (Fig. 9). The validation indicates that the model is able to predict reliable values for most environments, with an associated RMSE of 3.27 kg SOC m^{-3} and a ratio of performance to deviation (RPD), i.e. the ratio of the standard deviation to RMSE, of 2.89. Nevertheless, one can observe an underprediction of the model for some land use–soil type–depth increment combinations (Fig. 9). Two different environments for these outliers can be distinguished, i.e. on the one hand, subsoil horizons most likely containing peat and situated in moderately to very poorly drained soils, and on the other hand, Bh horizons enriched with organic matter (depth around 0.3–0.4 m) in well to moderately drained sandy podzols.

3.4. Model application — case study: SOC inventory Belgium

The estimated spatial distributions of SOC stocks in Flanders until reference depths of 0.3 and 1 m are calculated by combining the integrated form of the overall depth distribution model (Eq. (7)) with the PTF expressions (Eqs. (8)–(11)) and digital land use and soil type maps of the region (Figs. 10 and 11). Besides the importance of these maps regarding the understanding of current climate change process, they can be useful as input in estimating other important environmental threats, like potential groundwater contamination by pesticides or nitrate. As expected, the pattern of valleys and river systems can be recognised on both maps. The reduced oxidation capacity of SOC under anaerobic conditions results in remarkably higher carbon contents in the poorly drained valley and depression soils compared to the dry soils on the plateau (Meersmans et al., 2008). Moreover the clay rich soils in the coastal planes are characterised by high SOC densities. In these soils, organic matter is physically protected against degradation by microbial attack through sorption of organic matter to clay minerals and enclosure within the soil aggregates (Razafimbelo et al., 2008). While the map representing the SOC stock until 1 m depth (Fig. 11) is entirely dominated by soil type, the map showing SOC until a reference depth of 0.3 m (Fig. 10) also reflects the land use pattern. On this map, forested areas in the north-eastern part of the region as well as south to south-

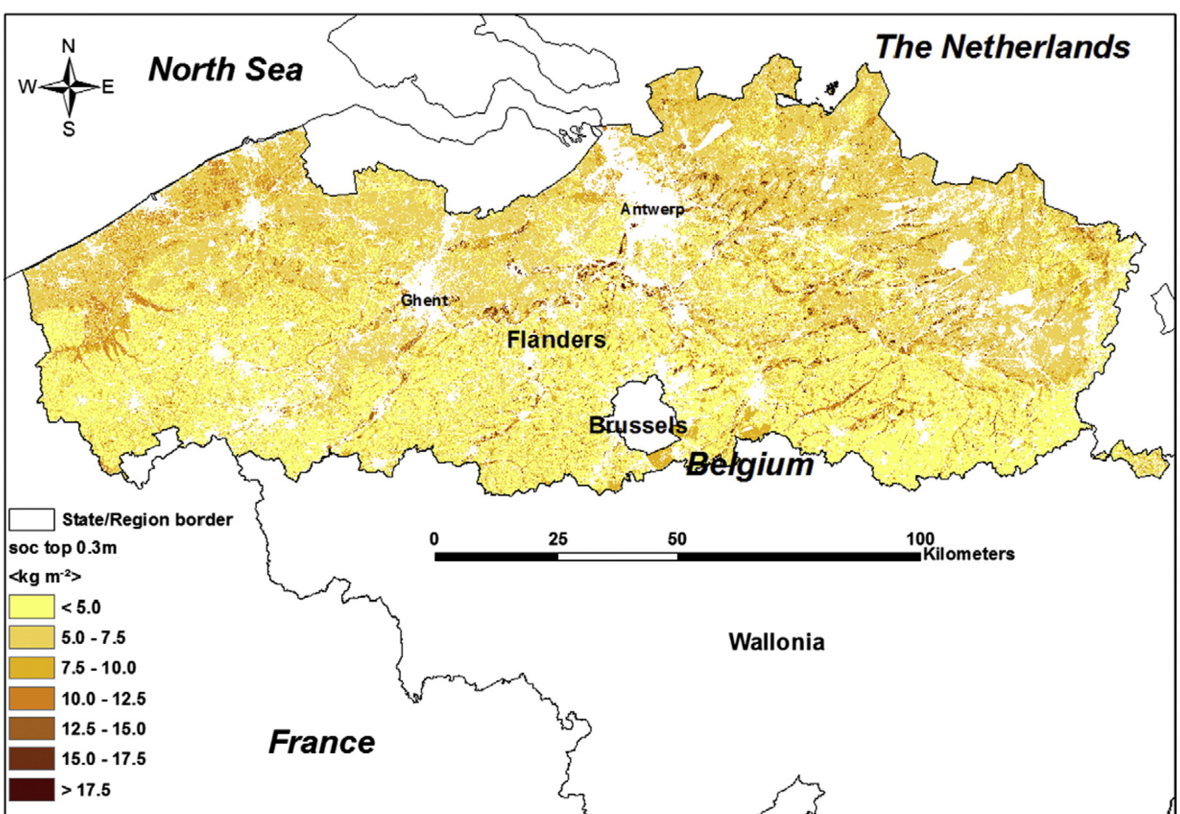

Fig. 10. SOC distribution map for Flanders (Belgium) for the top 0.3 m (kg m^{-2}).

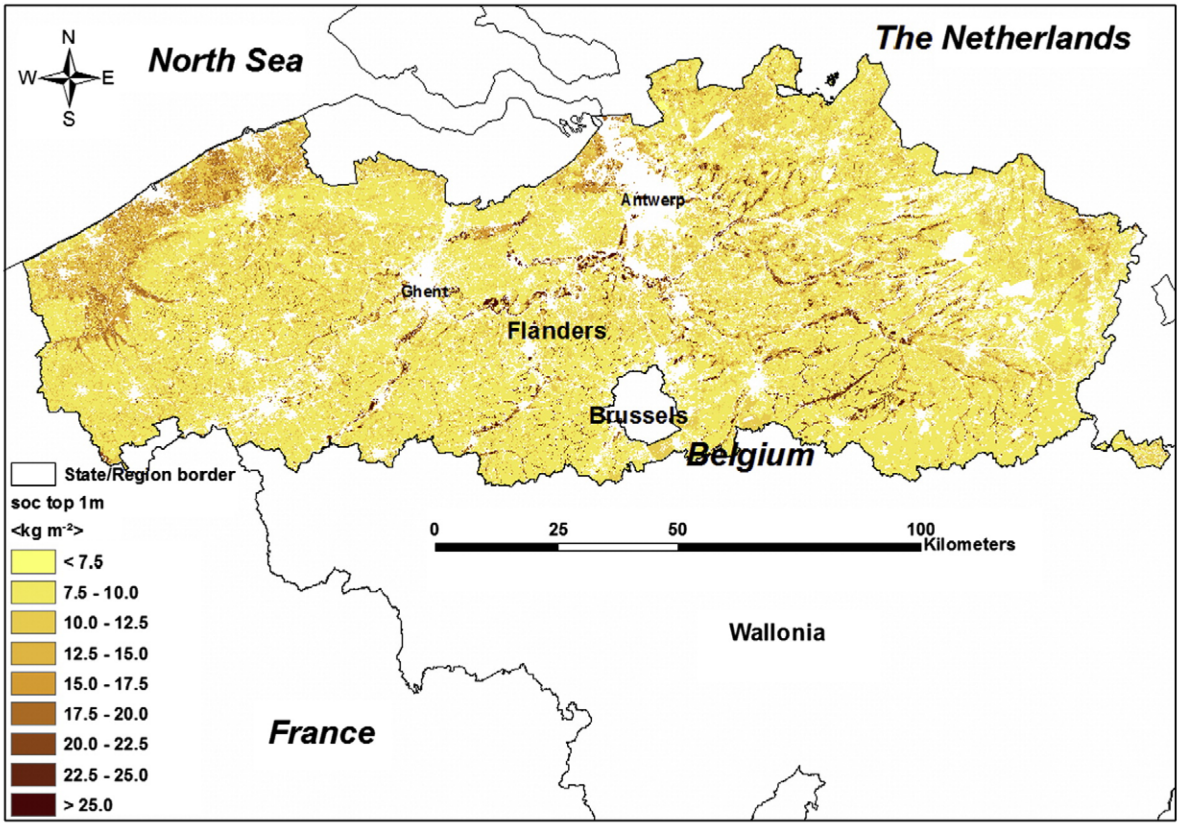

Fig. 11. SOC distribution map for Flanders (Belgium) for the top 1.0 m (kg m^{-2}).

east of Brussels can be easily recognised through their higher SOC densities in the topsoil. The white spots on the maps correspond to major cities (e.g. Antwerp and Ghent) or military areas where no soil type data is available. Consequently, only 77.1% of the total area of Flanders (i.e. 10,428 km^2) could be taken into account to calculate the total SOC stock for Flanders. The total SOC stocks for the corresponding area are estimated at 103.19 ± 1.27 Mt C until a reference depth of 1 m and 62.20 ± 0.72 Mt C until a reference depth of 0.3 m.

These results are in agreement with the ones obtained by Meersmans et al. (2008) using a multiple regression model for the top 1 m soil. These authors also pointed to the relation between the fluvial pattern and the spatial distribution of SOC in Flanders. Moreover the mean SOC mass densities by land use predicted following the present 3D model approach are comparable to the mean values for 1960 from studies following the common approach (i.e. calculating mean SOC stocks by landscape unit). The SOC mass density under grassland in this study (11.5 kg C m^{-2}) fits well in the range of mean values reported by other studies, e.g. Liebens and VanMolle (2003) (12.9 kg C m^{-2}) and Lettens et al. (2004) (11.7 kg m^{-2}), while the SOC mass density under cropland in this study (7.9 kg C m^{-2}) is situated in between the values obtained by Liebens and VanMolle (2003) (7.4 kg C m^{-2}) and Lettens et al. (2004) (8.9 kg C m^{-2}). All values are close to the overall mean SOC mass density value under cropland (7.8 kg C m^{-2}) reported for Flanders in 1990 by Sleutel et al. (2003).

4. Conclusions

The results of this study demonstrate that the SOC stock near the surface is determined by land use and soil type, while SOC near the bottom of the soil profile only depends on soil type (i.e. texture and drainage). Moreover, the interaction between texture and drainage has an important influence on the distribution of SOC with depth. In general, under grassland, increasing soil wetness results in higher SOC densities near the surface under sand and silt textured soils (Z, S, P, L, A) and into higher SOC densities at the bottom of the profile under silt and clay textured soils (U, E, A). Furthermore, under cropland higher clay content results in remarkable higher SOC contents throughout the profile in the poorly drained soils. The shape of the curve depends on the land use and texture. Under cropland, SOC remains constant in the tillage layer and is remarkably lower than at the same depths under grassland or forest. Tillage depth appears to be shallower in fine textured clay soils and tends to increase towards the sandy textured soil types, because in the latter ploughing was less limited by the traction in the 1960s (period of the database). Lower root to shoot ratios under forest compared to other land uses, resulting in a relative higher input of organic carbon by leaf fall (than at subsurface by roots), explain the more pronounced SOC declines with depth under forest than under grassland or cropland. Moreover, the SOC decline with depth is reduced when sand contents increase, suggesting that vertical transport of SOC is promoted in the more permeable sandy soils. The resulting SOC map for Flanders shows a strong correlation with the pattern of river valleys in the study area, as the poorly drained soils are characterised by high SOC contents. Furthermore, the clay rich soils in the coastal planes are also characterised by high SOC densities. The total SOC stock in the area is estimated at 62.20 ± 0.72 Mt C and 103.19 ± 1.27 Mt C for top 0.3 and 1 m of the soil, respectively. A future perspective can be to extend the present model to account for land use history or changed drainage conditions.

Acknowledgement

Research funded by a Ph.D. grant of the Institute for the Promotion of Innovation through Science and Technology in Flanders (IWT-Vlaanderen).

Appendix A. Supplementary data

Supplementary data associated with this article can be found, in the online version, at doi:10.1016/j.geoderma.2009.05.015.

References

Al-Adamat, R., Rawajfih, Z., Easter, M., Paustian, K., Coleman, K., Milne, E., Falloon, P., Powlson, D.S., Batjes, N.H., 2007. Predicted soil organic carbon stocks and changes in Jordan between 2000 and 2030 made using the GEFSOC modelling system. Agriculture Ecosystems and Environment 122 (1), 35–45.

Ameryckx, J.B., Verheye, W., Vermeire, R., 1995. Bodemkunde. Gent.

Andrews, S.S., Karlen, D.L., Cambardella, C.A., 2004. The soil management assessment framework: a quantitative soil quality evaluation method. Soil Science Society of America Journal 68 (6), 1945–1962.

Baisden, W.T., Parfit, R.L., 2007. Bomb C-14 enrichment indicates decadal C pool in deep soil? Biochemistry 85 (1), 59–68.

Balesdent, J., Chenu, C., Balabane, M., 2000. Relationship of soil organic matter dynamics to physical protection and tillage. Soil & Tillage Research 53 (3–4), 215–230.

Batjes, N.H., 2000. Effects of mapped variation in soil conditions on estimates of soil carbon and nitrogen stocks for South America. Geoderma 97 (1–2), 135–144.

Bhattacharyya, T., Pal, D.K., Easter, M., Batjes, N.H., Milne, E., Gajbhiye, K.S., Chandran, P., Ray, S.K., Mandal, C., Paustian, K., Williams, S., Killian, K., Coleman, K., Falloon, P., Powlson, D.S., 2007. Modelled soil organic carbon stocks and changes in the Indo-Gangetic Plains, India from 1980 to 2030. Agriculture Ecosystems and Environment 122 (1), 84–94.

Bohn, H.L., 1982. Estimate of organic-carbon in world soils 2. Soil Science Society of America Journal 46 (5), 1118–1119.

Boucneau, G., Van Meirvenne, M., Hofman, G., 1998. Comparing pedotransfer functions to estimate bulk density in northern Belgium. Pedologie — Themata 5, 67–70.

Cerri, C.E.P., Easter, M., Paustian, K., Killian, K., Coleman, K., Bernoux, M., Falloon, P., Powlson, D.S., Batjes, N.H., Milne, E., Cerri, C.C., 2007. Predicted soil organic carbon stocks and changes in the Brazilian Amazon between 2000 and 2030. Agriculture Ecosystems and Environment 122, 58–72.

Davidson, E.A., 1995. Spatial covariation of soil organic carbon, clay content and drainage class at a regional scale. Landscape Ecolology 10, 349–362.

Dawson, J.J.C., Godsiffe, E.J., Thompson, I.P., Ralebitso-Senior, T.K., Killham, K.S., Paton, G.I., 2007. Application of biological indicators to assess recovery of hydrocarbon impacted soils. Soil Biology & Biochemistry 39 (1), 164–177.

Don, A., Schumacher, J., Scherer-Lorenzen, M., Scholten, T., Schulze, E.D., 2007. Spatial and vertical variation of soil carbon at two grassland sites — implications for measuring soil carbon stocks. Geoderma 141, 272–282.

Dousset, S., Chauvin, C., Durlet, P., Thevenot, M., 2004. Transfer of hexazinone and glyphosate through undisturbed soil columns in soils under Christmas tree cultivation. Chemosphere 57 (4), 265–272.

Feller, C., Beare, M.H., 1997. Physical control of soil organic matter dynamics in the tropics. Geoderma 79 (1–4), 69–116.

Fontaine, S., Barot, S., Barré, P., Bdioui, N., Mary, B., Rumpel, C., 2007. Stability of organic carbon in deep soil layers controlled by fresh carbon supply. Nature 450, 277–280.

Gal, A., Vyn, T.J., Micheli, E., Kladivko, E.J., McFee, W.W., 2007. Soil carbon and nitrogen accumulation with long-term no-till versus moldboard plowing overestimated with tilled-zone sampling depths. Soil & Tillage Research 96, 42–51.

Gill, R., Burke, I.C., Milchunas, D.G., Lauenroth, W.K., 1999. Relationship between root biomass and soil organic matter pools in the shortgrass steppe of eastern Colorado. Ecosystems 2 (3), 226–236.

Gundersen, P., Callesen, I., de Vries, W., 1998. Nitrate leaching in forest ecosystems is related to forest floor C/N ratios. Environmental Pollution 102, 403–407.

Hilinski, T.E., 2001. Implementation of Exponential Depth Distribution of Organic Carbon in the CENTURY Model. www.nrel.colostate.edu/projects/century5/reference/html/Century/exp-c-distrib.htm.

Jackson, R.B., Schenk, H.J., Jobbagy, E.G., Canadell, J., Colello, G.D., Dickinson, R.E., Field, C.B., Friedlingstein, P., Heimann, M., Hibbard, K., Kicklighter, D.W., Kleidon, A., Neilson, R.P., Parton, W.J., Sala, O.E., Sykes, M.T., 2000. Belowground consequences of vegetation change and their treatment in models. Ecological Applications 10 (2), 470–483.

Jarvis, N., Larsbo, M., Roulier, S., Lindahl, A., Persson, L., 2007. The role of soil properties in regulating non-equilibrium macropore flow and solute transport in agricultural topsoils. European Journal of Soil Science 58 (1), 282–292.

Jobbagy, E.G., Jackson, R.B., 2000. The vertical distribution of soil organic carbon and its relation to climate and vegetation. Ecological Applications 10 (2), 423–436.

Jones, R.J.A., Hiederer, R., Rusco, E., Loveland, P., Montanarella, L., 2004. The map of organic carbon in topsoils in Europe, Version 1.2, September 2003: explanation of Special Publication Ispra 2004 No.72 (S.P.I.04.72). European Soil Bureau Research Report No.17. InOffice for Official Publications of the European Communities, Luxembourg.

Kamoni, P.T., Gicheru, P.T., Wokabi, S.M., Easter, M., Milne, E., Coleman, K., Falloon, P., Paustian, K., Killian, K., Kihanda, F.M., 2007. Evaluation of two soil carbon models using two Kenyan long term experimental datasets. Agriculture Ecosystems and Environment 122 (1), 95–104.

Kern, J.S., 1994. Spatial patterns of soil organic-carbon in the contiguous United States. Soil Science Society of America Journal 58 (2), 439–455.

Lafrance, P., Banton, O., 1995. Implication of spatial variability of organic-carbon on predicting pesticide mobility in soil. Geoderma 65 (3–4), 331–338.

Lettens, S., Van Orshoven, J., van Wesemael, B., Muys, B., 2004. Soil organic and inorganic carbon contents of landscape units in Belgium derived using data from 1950 to 1970. Soil Use and Management 20 (1), 40–47.

Lettens, S., van Orshoven, J., van Wesemael, B., Muys, B., Perrin, D., 2005. Soil organic carbon changes in landscape units of Belgium between 1960 and 2000 with reference to 1990. Global Change Biology 11 (12), 2128–2140.

Liebens, J., VanMolle, M., 2003. Influence of estimation procedure on soil organic carbon stock assessment in Flanders, Belgium. Soil Use and Management 19 (4), 364–371.

Lindahl, A.M.L., Kreuger, J., Stenström, J., Gärdenäs, A.I., Alavi, G., Roulier, S., Jarvis, N.J., 2005. Stochastic modeling of diffuse pesticide losses from a small agricultural catchment. Journal of Environmental Quality 34 (4), 1174–1185.

Manrique, L.A., Jones, C.A., 1991. Bulk density of soils in relation to soil physical and chemical properties. Soil Science Society of America Journal 55 (2), 476–481.

Meersmans, J., 2008. www.jeroenmeersmans.be/research/publications/depth3Dmod.

Meersmans, J., De Ridder, F., Canters, F., De Baets, S., Van Molle, M., 2008. A multiple regression approach to assess the spatial distribution of Soil Organic Carbon (SOC) at the regional scale (Flanders, Belgium). Geoderma 143 (1–2), 1–13.

Meersmans, J., van Wesemael, B., De Ridder, F., Fallas Dotti, M., De Baets, S., Van Molle, M., in press. Changes in organic carbon distribution with depth in agricultural soils in northern Belgium, 1960–2006. Global Change Biology. doi:10.1111/j.1365-2486.2009.01855.x.

Milne, E., Al Adamat, R., Batjes, N.H., Bernoux, M., Bhattacharyya, T., Cerri, C.C., Cerri, C.E.P., Coleman, K., Easter, M., Falloon, P., Feller, C., Gicheru, P., Kamoni, P., Killian, K., Pal, D.K., Paustian, K., Powlson, D.S., Rawajfih, Z., Sessay, M., Williams, S., Wokabi, S., 2007. National and sub-national assessments of soil organic carbon stocks and changes: the GEFSOC modelling system. Agriculture Ecosystems and Environment 122 (1), 3–12.

Mokany, K., Raison, R.J., Prokushkin, A.S., 2006. Critical analysis of root:shoot ratios in terrestrial biomes. Global Chang Biology 12, 84–96.

Ondersteunend Centrum GIS-Vlaanderen, 2001. Digital Soil Map of Flanders. VLM (Vlaamse Land Maatschappij), Brussels.

Ondersteunend Centrum GIS-Vlaanderen, 2002. Digital Land Use Map of Flanders. VLM (Vlaamse Land Maatschappij), Brussels.

Omonode, R.A., Vyn, T.J., 2006. Vertical distribution of soil organic carbon and nitrogen under warm-season native grasses relative to croplands in west-central Indiana, USA. Agriculture Ecosystems and Environment 117 (2–3), 159–170.

Pattison, A.B., Moody, P.W., Badcock, K.A., Smith, L.J., Armour, J.A., Rasiah, V., Cobon, J.A., Gulino, L.-M., Mayer, R., 2008. Development of key soil health indicators for the Australian banana industry. Applied Soil Ecology 40 (1), 155–164.

Poissant, L., Beauvais, C., Lafrance, P., Deblois, C., 2008. Pesticides in fluvial wetlands catchments under intensive agricultural activities. Science of the Total Environment 404 (1), 182–195.

Razafimbelo, T.M., Albrecht, A., Oliver, R., Chevallier, T., Chapuis-Lardy, L., Feller, C., 2008. Aggregate associated-C and physical protection in a tropical clayey soil under Malagasy conventional and no-tillage systems. Soil & Tillage Research 98 (2), 140–149.

Richards, J.E., Webster, C.P., 1999. Denitrification in the subsoil of the Broadbalk continuous wheat experiment. Soil Biology & Biochemistry 31 (5), 747–755.

Sleutel, S., De Neve, S., Hofman, G., 2003. Estimates of carbon stock changes in Belgian cropland. Soil Use and Management 19 (2), 166–171.

Slobodian, N., Van Rees, K., Pennock, D., 2002. Cultivation-induced effects on belowground biomass and organic carbon. Soil Science Society of America Journal 66 (3), 924–930.

Soil Survey Staff, 1951. Soil survey manual, United States Department of Agriculture. U.S. Dept. Agricultural Handbook, 18, Washington, D.C.

Tan, Z.X., Lal, R., Smeck, N.E., Calhoun, F.G., 2004. Relationships between surface soil organic carbon pool and dite variables. Geoderma 121, 187–195.

Trumbore, S., 2000. Age of soil organic matter and soil respiration: radiocarbon constraints on belowground C dynamics. Ecological Applications 10 (2), 399–411.

Van Meirvenne, M., Pannier, J., Hofman, G., Louwagie, G., 1996. Regional characterization of the long-term change in soil organic carbon under intensive agriculture. Soil Use Manage 12, 86–94.

Van Orshoven, J., Maes, J., Vereecken, H., Feyen, J., Didal, R., 1988. A structured database of Belgian soil profile data. Pedologie 38, 191–206.

Walkley, A., Black, I.A., 1934. An examination of Degtjareff method for determining soil organic matter and a proposed modification of the chromic acid titration method. Soil Science 37, 29–37.

Wang, S., Huang, M., Mickler, R.A., Li, K., Ji, J., 2004. Vertical distribution of soil organic carbon in China. Environmental Management 33, 200–209.

Zinn, Y.L., Lal, R., Resck, D.V.S., 2005. Texture and organic carbon relations described by a profile pedotransfer function for Brazilian Cerrado soils. Geoderma 127 (1–2), 168–173.